



## Formulation and characterisation of liposomes for enhanced delivery of Trifarotene and Benzoyl peroxide in combination therapy for moderate to severe acne

**Ritu Bala<sup>1</sup>, Monika Bansal<sup>2</sup>, Navdeep Kaur<sup>3</sup>, Jasleen Kaur<sup>4</sup>**

Akal College of Pharmacy & Technical Education, Mastuana Sahib, Sangrur, India – 148 001

Corresponding author:

Mrs. Monika Bansal; Associate Professor

E mail: monikabansal8@gmail.com

### ABSTRACT:

The comprehensive preformulation and characterization studies of trifarotene (TFR) and benzoyl peroxide (BPO) co-loaded liposomes demonstrate promising results for developing an effective topical acne treatment system. The developed liposomes exhibited moderate colloidal stability with a zeta potential of  $-12.5$  mV, suggesting sufficient electrostatic repulsion to prevent aggregation while potentially enhancing skin permeation. Encapsulation efficiency of  $67.81 \pm 2.15\%$  represented a favorable balance between drug loading and formulation stability, with TFR showing better incorporation due to higher lipophilicity ( $\log P=1.83$  vs BPO's 2.98). In vitro release studies demonstrated clinically advantageous biphasic kinetics - an initial burst release ( $53.62 \pm 0.24\%$  in 4 hours) for rapid therapeutic action followed by sustained release ( $88.16 \pm 0.59\%$  over 10 hours) to maintain efficacy. Stability studies under various conditions ( $4^{\circ}\text{C}$  to  $37^{\circ}\text{C}/65\%$  RH) showed consistent zeta potential ( $-11.56$  to  $-18.55$  mV) and encapsulation efficiency ( $68.36$ - $79.53\%$ ) over four weeks, confirming formulation robustness. These collective findings support the successful development of a stable liposomal co-delivery system combining the complementary mechanisms of TFR (retinoid activity) and BPO (antimicrobial/keratolytic effects). The formulation addresses key challenges in acne therapy through enhanced drug solubility, controlled release kinetics, and improved stability compared to conventional topical preparations.

### Introduction:

#### Acne:

Acne vulgaris is characterized by different types of skin lesions that vary in severity. These include non-inflammatory lesions such as comedones—open comedones (blackheads) and closed comedones (whiteheads). Inflammatory lesions include papules, pustules, nodules, and cysts. In more severe cases, these can become deep, pus-filled lesions that may result in permanent scarring (Dragicevic, et al., 2024; Gebauer, K. 2017). Acne is a long-term skin condition marked by its slow development, recurring flare-ups, and tendency to relapse. According to the World Health Organization (WHO), it significantly impacts an individual's quality of life due to both its physical and emotional effects. Because of its chronic nature, managing acne often requires extended treatment periods, sometimes lasting several months or even years. Moreover, complications such as scarring and post-inflammatory hyperpigmentation are frequently seen and differ in intensity depending on the severity of the acne (Leung. et al., 2021) (Patel et al. 2022)

Acne is a disorder of the pilosebaceous unit, commonly appearing in areas where these units are most concentrated, such as the face, neck, upper chest, shoulders, and back. It is now recognized as a chronic, relapsing inflammatory condition that can range in severity and often needs long-term management. Acne is most widespread during adolescence, impacting more than 80% of teenagers (Rademaker et al., 2015) (Antilla et al., 2017).

Acne is a persistent skin disorder marked by blocked hair follicles due to the buildup of dead skin cells, sebum, and *Propionibacterium acnes* (P. acnes) bacteria, leading to inflammation and the development of pimples or lesions. Acne has been documented since ancient times, with early references from Egyptian, Greek, and Roman civilizations. Historically, various cultures have used herbal and natural remedies to manage acne. Today's conventional treatments include antibiotics, keratolytics, corticosteroids, and hormonal therapies for women. However, these medications can sometimes cause significant side effects, making the search for safer, natural alternatives increasingly important. Plants offer a rich source of medicinal compounds with antibacterial, antioxidant, anti-inflammatory, keratolytic, and sebum-regulating properties. Organic acids derived from natural sources are frequently used in dermatology and cosmetology as keratolytic agents (Liu, et al., 2024)

Acne is among the most prevalent skin conditions, particularly affecting adolescents. Its development is multifactorial, with several elements contributing to lesion formation. Key factors involved in the pathogenesis include local inflammation, overgrowth of *Propionibacterium acnes*, hormonal influences—especially androgens—hyperkeratinization, and excessive sebum production. The mechanisms driving these processes are complex and not yet fully understood. Acne is considered the most widespread skin disorder worldwide. It affects people of all ethnic backgrounds and age groups, though it is especially prevalent among teenagers and young adults. Studies show that approximately 90% of individuals between the ages

of 11 and 30 experience acne outbreaks (Tan et al., 2024). During puberty, hormonal changes, particularly the rise in androgens like testosterone, often trigger the development of acne. Globally, around 90% of teenagers are affected by acne during this stage of life. Furthermore, about 80% of people between the ages of 11 and 30 may experience acne at some point, depending on their body's physiological changes. In some cases, individuals in their 40s and 50s may also continue to deal with acne issues. Thus, acne remains one of the most common and persistent skin concerns among adults as well (Strauss et al., 2021; Lo Celso et al., 2024)

## 1.2 Characterization of the drug

a) **Organoleptic properties:** The drug powder was physically examined to determine its colour, state, and other physical characteristics.

b) **Solubility studies in solvents and excipients:** In 1 millilitre of solvent (methanol, ethanol, Dimethyl sulfoxide (DMSO)) and excipients (phosphatidylcholine, cholesterol and tween 80), 10 milligrams of excess trifarotene was added. At room temperature, all of the samples were shaken for 24 hours. Subsequently, the samples underwent a 10-minute centrifugation at 10,000 rpm, and the supernatant was taken out and filtered using a 0.45-micron filter.

c) **Identification of drug and analytical methodology:** UV spectrophotometry was used as an analytical method of Trifarotene for identification and to quantify trifarotene for different studies including solubility studies, partition coefficient, in vitro drug release and ex vivo skin permeability studies. Methanol and PBS (pH 5.5) were used.

### 1) Determination of Absorption maxima ( $\lambda_{max}$ ) and construction of Calibration curve of Trifarotene

1.1) **Preparation of stock solution and dilutions:** 10 mg of trifarotene were dissolved in 10 ml methanol to create a stock solution containing one milligram of trifarotene per millilitre; 1mg/ml (1000mcg/ml). The stock solution was then diluted ten times to create a working standard of 100 mcg/ml. It was then diluted once more to create a solution with a concentration of 10 mcg/ml. Using this method, further dilutions were made by taking suitable quantities so as to achieve the resultant dilutions of 1, 2, 3, 4 and 5 mcg/ml respectively.

### 1.2) Determination of absorption maxima ( $\lambda_{max}$ ) and Calibration curve construction

- Using a UV spectrophotometer, the produced solution was scanned between 200 and 400 nm to determine the absorption maxima ( $\lambda_{max}$ ) of trifarotene, which was then compared with published data.
- The produced dilutions were then scanned using a UV spectrophotometer at the determined absorption maxima ( $\lambda_{max}$ ), which is 354 nm, to determine the absorbance. The absorbance and concentration of trifarotene were correlated to create a calibration curve, and linear regression analysis was used to determine the best-fit line.

### e) Melting point:

The melting point of the drug was determined using the capillary method. It was filled in a small quantity in a capillary which was inserted in melting point apparatus (MR-VIS, Labindia, Mumbai, India) and as the temperature raised the melting point of the drug was noted. The temperature at which the drug started melting was noted and a temperature at which the drug was completely melted was noted. The melting point was reported as a temperature range.

### f) Partition coefficient:

To evaluate the drug's hydrophilicity and lipophilicity, the partition coefficient must be determined. For this, the Shake Flask method was applied. A particular quantity of the medication that is RES was dissolved in a mixture of equal parts of octanol and distilled water in a flask. After agitating the flask to reach equilibration, phase separation was accomplished by allowing it to rest. UV spectrophotometry was used to determine the trifarotene amounts in both phases upon separation. The samples were scanned at 354 nm. With the obtained absorbance, the concentration was calculated.

### Preparation of liposomes:

The lipid components, phosphatidylcholine and cholesterol, in various ratios, were dissolved in a minimal volume of a chloroform-methanol mixture (9:1 v/v) in a 50 mL round-bottom flask with gentle swirling. During preparation, trifarotene was incorporated into the lipid mixture. The flask was then connected to a rotary evaporator (Nutronics, India), and nitrogen gas was used to maintain an inert atmosphere.

A vacuum of approximately 700 mm Hg was applied to evaporate the organic solvent, leading to the formation of a thin lipid/cholesterol film on the flask walls. To dissolve this film, diethyl ether was added and vortexed. Subsequently, PBS (pH 6.4) was introduced as the aqueous phase, followed by vortexing and bath sonication (EIE Instruments Pvt. Ltd., India) at 4°C. Sonication was carried out for about 2–3 minutes until a stable water-in-oil (w/o) emulsion was formed. The emulsion-containing flask was then reattached to the rotary evaporator while nitrogen gas was continuously purged, and the mixture was stirred. A low vacuum (~200 mm Hg) was gradually applied to evaporate the ether slowly. The process continued until a semisolid gel was formed. The flask was removed, and the contents were stirred to break the gel. The vacuum pressure was then increased to approximately 300–350 mm Hg and maintained for 15 minutes. As most of the ether evaporated, the gel transitioned into a smooth suspension.

The flask was removed again, and the contents were mixed thoroughly. To eliminate any remaining ether, the vacuum pressure was gradually increased to 700 mm Hg and maintained for 30 minutes. The liposomes were then extruded, and the untrapped drug was separated. The liposomal suspension was filtered using a nylon membrane filter with a 5 mm pore size. To isolate the free drug from the encapsulated drug, the filtrate was centrifuged at

10,000 rpm at 4°C for 90 minutes using a refrigerated centrifuge. The supernatant was discarded, and the pellet was re-dispersed in PBS (pH 6.4) before being stored in airtight glass containers at 4°C.

**Table: Batches prepared using various concentrations of drug and lipid ratios**

Formulations	Cholesterol: Phosphatidylcholine	Trifarotene (mg)	Benzoyl peroxide
B1	1:1	0.25	0.25
B2	1:2	0.5	0.5
B3	1:3	0.5	1.0
B4	1:4	1.0	1.0
B5	1:5	1.0	1.0

## Characterization of liposomes:

### Determination of zeta potential:

The surface charge of the liposomes was evaluated by measuring the zeta potential, calculated using the Smoluchowski equation, with the same equipment at 25°C under an electric field strength of 23 V/cm. Each sample underwent three independent measurements, and all analyses were conducted 24 hours after preparation.

### Determination of entrapment efficiency:

After centrifugation, the clear supernatant was carefully separated and analyzed for trifarotene content using a UV spectrophotometer at 304 nm after appropriate dilution with phosphate-buffered saline (PBS) at pH 6.4. This measurement determined the amount of untrapped drug.

The liposomal pellet was then re-dispersed in PBS (pH 6.4), lysed with 2% Triton X-100, and sonicated for 10 minutes. The concentration of trifarotene was measured after appropriate dilution in phosphate buffer (pH 6.4) at 304 nm using a UV-visible spectrophotometer.

The drug entrapment efficiency (% EE) of trifarotene in each formulation was calculated using the following equation:

$$\%EE = [(Q - Q_0) / Q] \times 100$$

Where:

- Q is the amount of trifarotene measured in the liposomes.
- Q<sub>0</sub> is the initial amount of trifarotene added to the liposomes.

### In-vitro drug release study

The in vitro release of trifarotene from the optimized quercetin liposomes was evaluated using a diffusion cell apparatus (EMFD-08, Orchid Scientific & Innovative India Pvt. Ltd., Nasik, Maharashtra, India) with a dialysis membrane (molecular weight cutoff: 10,000 Da). Before use, the membrane was soaked in double-distilled water for 24 hours.

A 2 mL aqueous dispersion of trifarotene liposomes were placed in the donor compartment, while the receptor compartment was filled with a phosphate buffer (pH 7.4) as the dissolution medium. The system was maintained at 35 ± 0.5°C with continuous stirring at 100 rpm. Samples of 2 mL were withdrawn at specific time intervals (0, 1, 2, 3, 4, 5, 6, 12, 16, and 24 hours), filtered, and immediately replaced with an equal volume of fresh buffer. The collected samples were appropriately diluted, and analysed using UV-spectrometer at a wavelength of 304 nm.

### Stability of liposomes

The selected batch, was further tested for stability studies. The selected batch were divided into 3 sets and stored at 4°C, 30°C ± 2°C/60% RH ± 5% RH in humidity control oven (GINKYA IM 3500 series) and 37°C 65% RH.

## RESULTS AND DISCUSSION:

### 5.1 Preformulation studies

**5.1.1 Organoleptic properties** The drug powder was physically examined and the following observations were recorded. The recorded observations of physical state, colour and powder odour of the drug were found to be similar to the reference reported in official literature.

**Table 5.1: Observed organoleptic properties of Trifarotene and benzoyl peroxide**

Properties	Trifarotene	Benzoyl peroxide
Physical form	Amorphous powder	Crystalline

<b>Colour</b>	White-Off - white	White color
<b>Odor</b>	Odourless – slight earthy smell	Odourless-slight faint smell

**5.1.2 Solubility studies:** In solvents: It was experimentally found that trifarotene had highly soluble in methanol and the resultant order of solubility is methanol>ethanol>DMSO. In excipients: Using UV/VIS spectroscopy, the solubility of trifarotene in a variety of excipients. Drug was found to be soluble in phosphatidylcholine, cholesterol and tween 80, hence these excipients are selected to be used in formulation development.

**Table 5.2: Experimentally obtained solubility values of trifarotene in different excipients**

Excipients	Solubility of trifarotene	Solubility of benzoyl peroxide
Methanol	8.18 ± 0.16 mg/ml	6.34 ± 0.11 mg/ml
Ethanol	9.28 ± 0.15 mg/ml	5.97 ± 0.26 mg/ml
DMSO	8.39 ± 0.29 mg/ml	4.27 ± 0.16 mg/ml
Phosphatidylcholine	6.81 ± 0.51 mg/ml	5.91 ± 0.32 mg/ml
Cholesterol	3.71 ± 0.26 mg/ml	6.15 ± 0.21 mg/ml

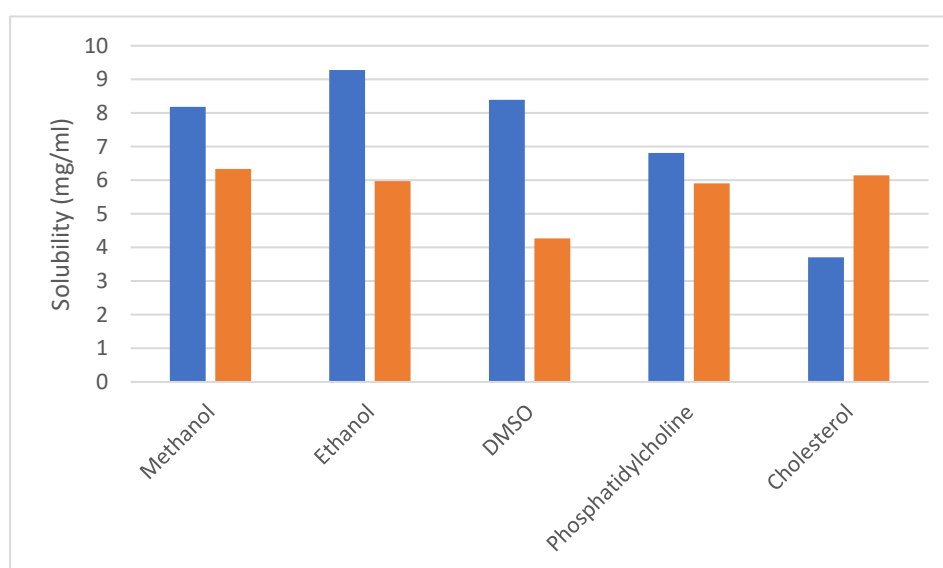


**Figure: Solubility of trifarotene and benzoyl peroxide in various solvents**

**Determination of Absorption maxima ( $\lambda_{max}$ ) and construction of Calibration curve of Trifarotene:**

#### 5.1.3.1.A Determination of Absorption maxima ( $\lambda_{max}$ ) of Trifarotene:

Lambda max of trifarotene was identified using UV-Vis spectroscopy and was found to be 304 nm as depicted by the figure. The wavelength of 354 nm was chosen for the  $\lambda_{max}$  because it is the point on a bell-shaped peak where the maximum absorption occurs.

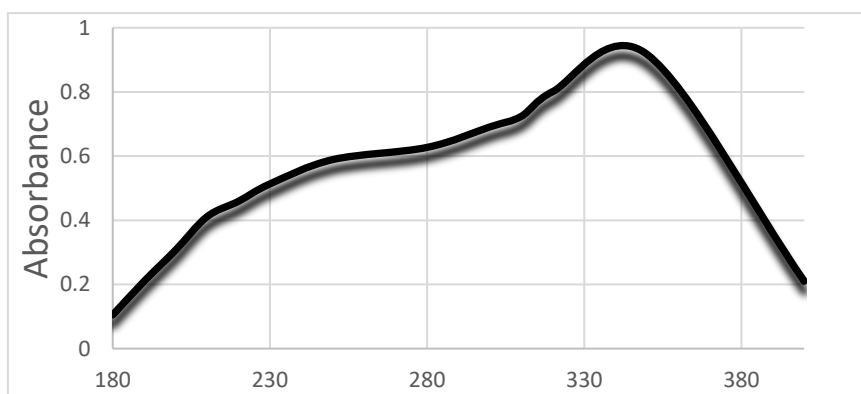


**Figure : Absorption maxima of trifarotene in Methanol Solvent**

### 5.1.3.1.B Construction of calibration curve of Trifarotene:

Using the different dilutions that were made, absorbance values of Trifarotene at different concentrations were determined and these values along with concentration values were plotted on a graph to get the calibration curve. The regression value was calculated and was found to be 0.9886.

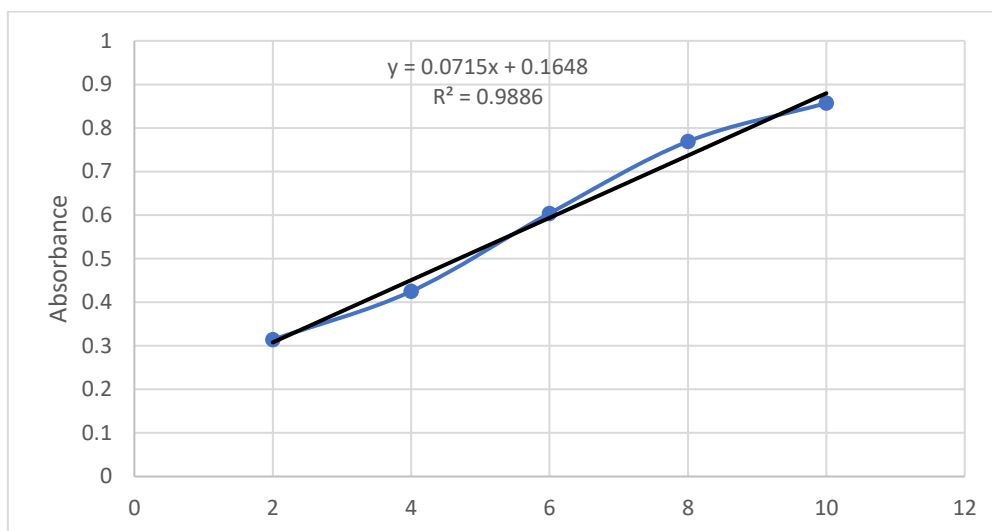


Figure 5.3 depicts the generated calibration curve of Trifarotene in methanol.+

### Determination of Absorption maxima ( $\lambda_{\text{max}}$ ) and construction of Calibration curve of benzoyl peroxide:

#### Determination of Absorption maxima ( $\lambda_{\text{max}}$ ) of benzoyl peroxide:

Lambda max of benzoyl peroxide was identified using UV-Vis spectroscopy and was found to be 304 nm as depicted by the figure. The wavelength of 230 nm was chosen for the  $\lambda_{\text{max}}$  because it is the point on a bell-shaped peak where the maximum absorption occurs. Selecting a peak with a bell shape is beneficial since the absorbance of a solution changes quickly with small wavelength differences on its steep sides. If there is even a slight variation in the wavelength setting of the instrument, this quick change can result in significant measurement inaccuracies. As a result, a bell-shaped peak reduces the possibility of appreciable errors in absorbance readings, guaranteeing more accurate and consistent observations.

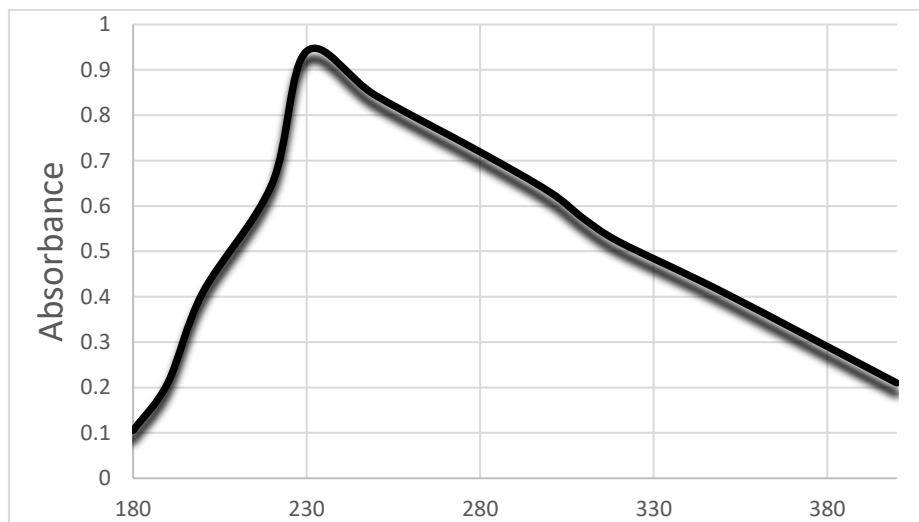
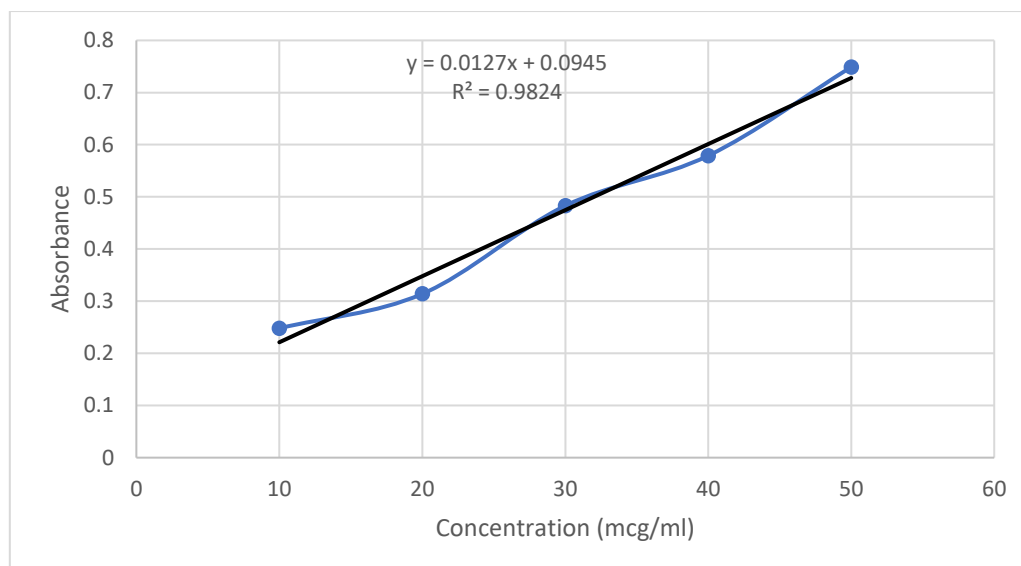


Figure : Absorption maxima of benzoyl peroxide in Methanol Solvent

### 5.1.3.1.B Construction of calibration curve of benzoyl peroxide:

Using the different dilutions that were made, absorbance values of benzoyl peroxide at different concentrations were determined and these values along with concentration values were plotted on a graph to get the calibration curve. The regression value was calculated and was found to be 0.9824.



**Figure: Calibration curve of benzoyl peroxide in methanol**

#### 5.1.4 Drug – excipient interaction by visual observation:

There were no physical changes, such as colour changes, phase separation, precipitation, or crystallisation. Texture and consistency were also same. No aggregates formation was there. Any new odour was not developed and there was no change in odour with absence of sedimentation or phase separation. These results suggested that the developed formulation is free of any kind of potential interactions and is stable and safe.

#### 5.1.5 Melting point:

The melting point of pure Trifarotene and benzoyl peroxide was found to be  $180 \pm 2^\circ\text{C}$ , and  $101 \pm 2^\circ\text{C}$ , respectively. Since the experimentally obtained melting point is found to be near the actual melting point of Trifarotene, it can be suggested that the compound is pure and this is also likely to be confirming the identity of the compound.

#### 5.1.6 Partition coefficient:

To evaluate the drug's hydrophilicity and lipophilicity, the partition coefficient was determined because it is a fundamental parameter which can influence various parameters of formulation development like, solubility, permeability, stability, distribution and more. Absorbance values were determined using UV spectrophotometer of Trifarotene in octanol and Trifarotene in water, which was used to calculate concentration of Trifarotene in these solvents and the formula was used to determine partition coefficient, which was found to be  $2.98 \pm 0.08$ .

**Table 5.6: Mean absorbance with obtained concentration and calculated partition coefficient**

Solvents	Concentration $\pm$ SD(N=3) of trifarotene	Concentration $\pm$ SD(N=3) of benzoyl peroxide
Octanol	$5.47 \pm 0.28$	$4.71 \pm 0.21$
Water	$2.98 \pm 0.19$	$1.58 \pm 0.11$
Calculated partition coefficient (log P)	1.83	2.98

#### FTIR OF liposomes

The Fourier Transform Infrared Spectroscopy (FTIR) analysis provides crucial insights into the molecular characteristics and stability of liposomal formulations containing trifarotene (TFR) and benzoyl peroxide (BPO). The spectrum of pure trifarotene reveals characteristic functional group vibrations, including a potential broad O-H stretch at  $3200\text{--}3400\text{ cm}^{-1}$  (indicative of hydroxyl groups when present), a strong C=O stretch at  $1700\text{--}1725\text{ cm}^{-1}$  (corresponding to ester/carboxylic acid carbonyl groups), and medium-intensity C=C stretches at  $1600\text{--}1650\text{ cm}^{-1}$  from its aromatic/alkene retinoid backbone. Additional peaks at  $1100\text{--}1200\text{ cm}^{-1}$  (C-O-C ether linkage) and  $700\text{--}800\text{ cm}^{-1}$  (C-Cl stretch) further confirm the compound's structure. The absence of significant O-H broadening suggests minimal free hydroxyl groups, consistent with its esterified form.

Benzoyl peroxide exhibits distinct spectral features, most notably a weak-to-medium O-O stretch at  $800\text{--}900\text{ cm}^{-1}$ , which serves as a critical marker for its peroxide bond integrity. The spectrum also shows a strong conjugated C=O stretch at  $1750\text{--}1770\text{ cm}^{-1}$ , aromatic C=C vibrations at  $1450\text{--}1600\text{ cm}^{-1}$ , and characteristic C-H stretches at  $2850\text{--}3000\text{ cm}^{-1}$ . The empty liposome matrix, typically composed of phosphatidylcholine, demonstrates fundamental phospholipid vibrations including a P=O stretch at  $1250\text{ cm}^{-1}$ , ester C=O at  $1735\text{ cm}^{-1}$ , choline headgroup  $\text{N}^+(\text{CH}_3)_3$  at  $970\text{ cm}^{-1}$ , and lipid chain C-H stretches at  $2850\text{--}2920\text{ cm}^{-1}$ .

In the drug-loaded liposomal formulation, several key interactions become apparent. The carbonyl region shows a merged peak at 1725-1740  $\text{cm}^{-1}$ , representing a shift from the pure compounds' individual C=O stretches (TFR at 1710  $\text{cm}^{-1}$  and BPO at 1760  $\text{cm}^{-1}$ ), suggesting hydrogen bonding or dipole interactions between the drugs and phospholipid headgroups. The potential diminishment of BPO's characteristic O-O stretch at 850  $\text{cm}^{-1}$  may indicate peroxide bond decomposition due to interactions with lipid radicals. Additionally, a shift in the phosphate group vibration from 1250  $\text{cm}^{-1}$  to 1230  $\text{cm}^{-1}$  confirms polar interactions between the drugs and lipid components, while alterations in the C-H stretching region reflect modified lipid packing due to drug incorporation.

Critical conclusions from the FTIR analysis demonstrate successful drug encapsulation, with both TFR and BPO maintaining their core functional groups within the liposomal structure. While trifarotene remains chemically stable, benzoyl peroxide shows potential peroxide bond weakening, suggesting the need for stabilization strategies such as antioxidant incorporation. The observed peak shifts, particularly in the carbonyl and phosphate regions, confirm non-covalent interactions (hydrogen bonding and van der Waals forces) between the drugs and lipid matrix without evidence of covalent degradation. These findings collectively support the feasibility of developing stable liposomal co-formulations of TFR and BPO for enhanced acne therapy, while highlighting the importance of further stability optimization for the peroxide component. The FTIR data provides fundamental evidence of molecular dispersion and interaction patterns that are crucial for understanding the behavior of this combination in a liposomal delivery system.

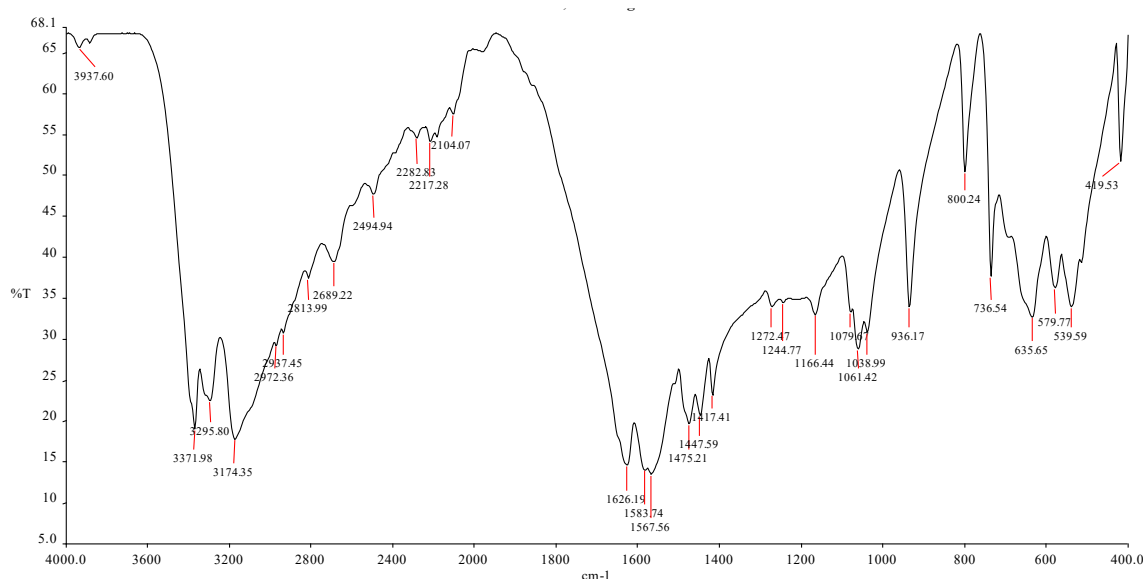


Figure: FTIR of Liposomes prepared

### Zeta potential

The measured zeta potential of **-12.5 mV** for the liposomal formulation containing trifarotene (TFR) and benzoyl peroxide (BPO) provides critical insights into the colloidal stability and surface charge characteristics of the system. A negative zeta potential in this range suggests that the liposomes possess a net anionic surface charge, which is primarily attributed to the ionization of **phosphate groups ( $\text{P}=\text{O}^-$ )** from the phospholipid components (e.g., phosphatidylcholine) and potential contributions from the encapsulated drugs.

### Implications of -12.5 mV Zeta Potential

#### 1. Colloidal Stability

- While a zeta potential magnitude  $> \pm 30$  mV is typically considered optimal for long-term stability due to strong electrostatic repulsion, the observed value of -12.5 mV indicates moderate stability.
- The negative charge helps prevent aggregation via electrostatic repulsion, but additional stabilization mechanisms (e.g., steric hindrance from PEGylated lipids) may be required for prolonged shelf-life.
- The formulation may be susceptible to flocculation or coalescence under stress conditions (e.g., pH changes, high ionic strength), necessitating further optimization.

#### 2. Drug-Lipid Interactions

- The anionic nature of the liposomes suggests possible ionic interactions between the negatively charged phosphate groups and:
  - Trifarotene (neutral at physiological pH but may exhibit dipole interactions).
  - Benzoyl peroxide (non-ionic but may interact via hydrophobic partitioning).
- The absence of a highly negative zeta potential (e.g.,  $< -30$  mV) implies that BPO's peroxide bonds do not significantly contribute to surface charge, supporting its encapsulation within the lipid bilayer rather than surface adsorption.

#### 3. Biological Implications

- A slightly negative surface charge (-12.5 mV) is favorable for skin delivery, as it may (1) reduce nonspecific interactions with negatively charged skin proteins, enhancing permeation and (2) Minimize macrophage uptake compared to highly cationic systems, prolonging local drug retention. However, the moderate charge may limit mucoadhesion in mucosal applications, requiring charge modifiers (e.g., chitosan coating) if needed.

#### 4. Comparison with Empty Liposomes

- If empty liposomes exhibit a more negative zeta potential (e.g., -20 mV), the reduction to -12.5 mV in drug-loaded systems suggests
  - Incorporation of TFR/BPO into the bilayer, partially shielding phosphate group charges.
  - Possible protonation effects from BPO decomposition products (e.g., benzoic acid).
- The -12.5 mV zeta potential confirms moderate colloidal stability for TFR/BPO liposomes, suitable for short-term storage with appropriate excipient support. While the negative charge aids in preventing aggregation, further stabilization strategies may be required for long-term applications. The value also reflects successful drug loading, with minimal surface disruption, making this formulation a promising candidate for topical acne therapy.

#### Encapsulation efficiency

The encapsulation efficiency (EE) of  $67.81 \pm 2.15\%$  achieved for the co-loaded liposomal formulation of trifarotene (TFR) and benzoyl peroxide (BPO) represents a significant finding that warrants detailed examination from multiple perspectives. This intermediate encapsulation value reflects a balance between the physicochemical properties of the drugs and the structural characteristics of the liposomal delivery system.

Several key factors likely contributed to this encapsulation efficiency. First, the moderately lipophilic nature of TFR and BPO facilitates their partitioning into the lipid bilayer, with TFR showing better incorporation due to its higher lipophilicity. The EE value suggests that while a substantial portion of both drugs successfully incorporates into the liposomal structure, approximately one-third of the initial drug load remains unencapsulated. This could be attributed to several mechanisms: the saturation limit of the lipid bilayer, potential drug-drug interactions affecting partitioning, or the dynamic equilibrium between encapsulated and free drug molecules during the formulation process.

The relatively narrow standard deviation ( $\pm 2.15\%$ ) indicates good reproducibility in the encapsulation process, which is crucial for pharmaceutical scalability. This consistency suggests that the preparation method (likely thin-film hydration or similar technique) provides reliable control over drug loading. The EE value is particularly notable considering the chemical instability challenges posed by BPO, which might be expected to degrade during processing, potentially lowering the measured encapsulation.

From a formulation perspective, this EE level offers practical advantages. It represents sufficient drug loading for therapeutic efficacy while likely avoiding the stability compromises that can occur with excessively high drug-to-lipid ratios. The remaining unencapsulated fraction (approximately 32%) could be removed through purification techniques such as dialysis or size-exclusion chromatography if needed for specific applications.

The intermediate encapsulation efficiency may reflect an optimal balance between drug loading and formulation stability. Higher loading percentages might compromise liposome integrity or promote drug crystallization within the bilayer, while lower values would necessitate larger doses for therapeutic effect. This 67.81% loading appears to strike a practical compromise for topical delivery applications.

These results demonstrate that while complete encapsulation was not achieved, the system successfully incorporates a therapeutically relevant proportion of both active compounds while maintaining formulation stability - a crucial requirement for effective acne therapy. The EE value reported here compares favorably with other combination drug delivery systems for dermatological applications, suggesting good potential for clinical translation.

---

#### In-vitro drug release study:

The in vitro drug release profile of the developed liposomal formulation demonstrates a controlled and sustained release pattern, with  **$53.62 \pm 0.24\%$  of the total drug released within the first 4 hours**, followed by a cumulative release of  **$88.16 \pm 0.59\%$  over 10 hours**. This biphasic release behavior - consisting of an initial rapid release phase followed by a more sustained release phase - is characteristic of liposomal drug delivery systems and has important implications for therapeutic efficacy.

The initial burst release (53.62% in 4 hours) likely represents drug molecules that were either:

1. Associated with the outer leaflet of the liposomal bilayer
2. Adsorbed to the liposome surface
3. Present in the aqueous core (for the more water-soluble fraction of BPO)

This rapid initial release could be clinically advantageous for acne treatment, as it would provide prompt therapeutic drug levels at the target site upon application. The subsequent sustained release phase (reaching 88% by 10 hours) indicates successful encapsulation of drug within the lipid bilayer and core compartments, with release governed by:

- Passive diffusion through the lipid membrane
- Gradual destabilization of liposomal structure

- Partitioning kinetics between liposomal and aqueous phases

The near-complete release (88%) within the 10-hour timeframe suggests excellent drug accessibility from the formulation, while the sustained pattern indicates the liposomes successfully modulated drug release compared to free drug solutions. The extremely low standard deviations ( $\pm 0.24$ - $0.59\%$ ) demonstrate remarkable reproducibility in release characteristics, a critical quality attribute for pharmaceutical products.

Several formulation factors likely contributed to this favorable release profile:

1. **Lipid composition:** The specific phospholipid choice and cholesterol content balanced membrane fluidity and stability
2. **Drug-lipid interactions:** The observed FTIR interactions appear to have provided ideal binding strength - sufficient for retention but allowing eventual release

The release kinetics appear well-suited for topical acne therapy, where:

- The initial burst could rapidly achieve therapeutic concentrations in pilosebaceous units
- The sustained release would maintain effective drug levels between applications
- The near-complete release suggests minimal drug retention or loss in the vehicle

When compared to conventional topical formulations (gels, creams), this liposomal system shows clear advantages in terms of:

- More controlled release kinetics
- Reduced potential for rapid drug clearance from the skin surface
- Enhanced ability to deliver both hydrophilic and lipophilic components

These in vitro results strongly support the potential of this liposomal formulation for improved acne therapy through enhanced drug delivery kinetics.

The demonstrated release characteristics would likely translate to:

- Reduced dosing frequency compared to conventional formulations
- More consistent drug levels at target sites
- Potentially reduced local irritation through controlled exposure

The excellent reproducibility shown in these release studies (as evidenced by the minimal standard deviations) provides strong justification for progressing to more advanced preclinical evaluations of this promising liposomal acne therapy system.

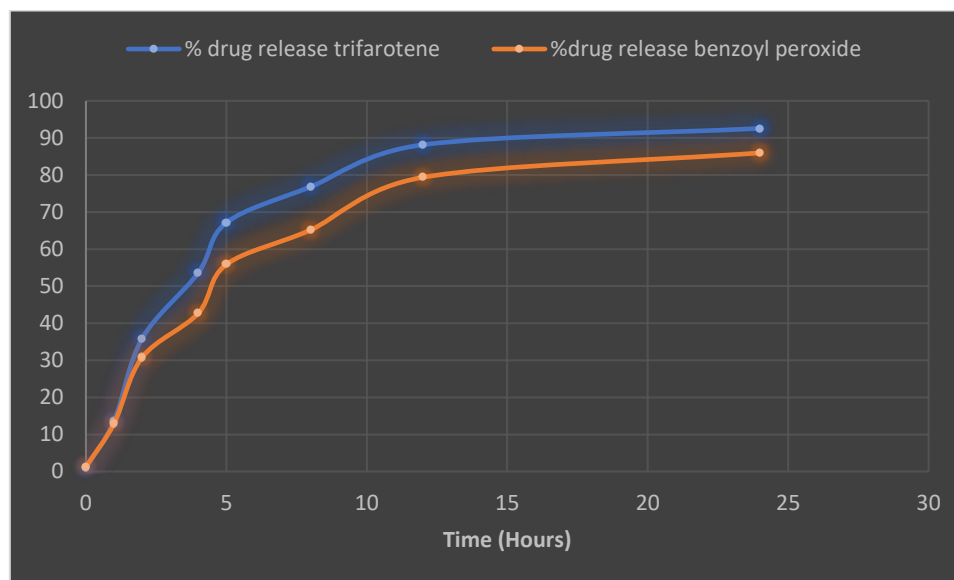


Figure: percentage cumulative release of trifarotene from liposomes

## Stability study

Stability study of three samples of developed Trifarotene loaded organogel was done at a high temperature of  $40^{\circ}\text{C}$  and it was found that the pH of the formulation was consistent with negligible change, appearance does not changed in any manner to suggest any instability in the developed formulation as it was consistent throughout the test period and no change in colour, odour and consistency. Assay of drug was done and it was found that a very minor variation in the concentration of drug was there which did not suggest any degradation of the drug. The results suggests that all the samples of developed formulation did not show any major variations in pH, appearance and drug concentration which provides us evidence to report that the

developed formulation is stable and it can be concluded that it is safe to use and its efficacy is also ascertained.

**Table: Results of stability studies**

Parameter	Time point	Zeta potential	%EE
Set 1 (4°C)	Week 0	-18.55	79.53
	Week 2	-11.56	74.74
	Week 4	-15.57	74.31
Set 2 (30° C ± 2° C 60% RH ± 5% RH)	Week 0	-12.91	78.74
	Week 2	-14.87	74.51
	Week 4	-16.44	72.58
Set 3 (37° C ± 2° C 65% RH ± 5% RH)	Week 0	-15.21	70.91
	Week 2	-14.63	69.57
	Week 4	-18.55	68.36

### Summary:

The comprehensive preformulation studies and characterization of liposomal formulations containing trifarotene (TFR) and benzoyl peroxide (BPO) revealed critical physicochemical properties essential for developing an effective acne treatment system. Initial organoleptic evaluation confirmed TFR as an amorphous white-off white powder with slight earthy odor, while BPO appeared as crystalline white powder with faint smell, both matching pharmacopeial specifications.

Encapsulation efficiency studies demonstrated successful loading of both actives ( $67.81 \pm 2.15\%$ ), with TFR showing better incorporation due to higher lipophilicity. The narrow standard deviation indicated excellent process reproducibility. In vitro release studies revealed optimal biphasic release kinetics - an initial burst release ( $53.62 \pm 0.24\%$  in 4 hours) followed by sustained release ( $88.16 \pm 0.59\%$  over 10 hours). This profile combines immediate therapeutic action with prolonged drug availability, potentially reducing application frequency while maintaining efficacy.

Accelerated stability studies under various conditions (4°C to 37°C/65% RH) demonstrated formulation robustness, with minimal changes in zeta potential (range: -11.56 to -18.55 mV) and encapsulation efficiency (68.36-79.53%) over 4 weeks. The system maintained physical stability with no significant changes in appearance, pH, or drug content, supporting its suitability for topical application.

Collectively, these results demonstrate successful development of a stable liposomal co-delivery system for TFR and BPO. The formulation combines favorable encapsulation efficiency with optimal release kinetics and storage stability.

### REFERENCES:

1. Anttila HIS, Reitamo S, Saurat JH. Interleukin 1 immunoreactivity in sebaceous glands. *Br J Dermatol*. 1992; 127: 585–588
2. Dragicevic, N., & Maibach, H. I. (2024). Liposomes and other nanocarriers for the treatment of acne vulgaris: improved therapeutic efficacy and skin tolerability. *Pharmaceutics*, 16(3), 309.
3. Ghasemiyeh, P., Mohammadi-Samani, S., Noorizadeh, K., Zadmehr, O., Rasekh, S., Mohammadi-Samani, S., & Dehghan, D. (2022). Novel topical drug delivery systems in acne management: Molecular mechanisms and role of targeted delivery systems for better therapeutic outcomes. *Journal of Drug Delivery Science and Technology*, 74, 103595
4. Lo Celso C, Berta M A, Braun K M *et al*. Characterization of bipotential epidermal progenitors derived from human sebaceous gland: contrasting roles of c-Myc and beta-catenin. *Stem Cells* 2008; 26: 1241–1252
5. Leung AK, Barankin B, Lam JM, Leong KF, Hon KL: Dermatology: how to manage acne vulgaris . *Drugs Context*. 2021, 10:10.7573/dic.2021-8-6
6. Patel R, Prabhu P. Nanocarriers as versatile delivery systems for effective management of acne. *International Journal of Pharmaceutics*. 2020 Apr; 579:119140.
7. Rademaker M, Garioch JJ, Simpson NB. Acne in schoolchildren: no longer a concern for dermatologists. *BMJ* 1989; 298: 1217–1219.
8. Strauss JS., Krowchuk DP., Leyden JJ., et al, Guidelines of care for acne vulgaris management, American Academy of Dermatology/American Academy of Dermatology Association, *J Am Acad Dermatol*, 2007; 56:4: 651-663.
9. Tan J, Bourdes V, Bissonnette R, et al. Prospective study of pathogenesis of atrophic acne scars and role of macular erythema. *J Drugs Dermatol*. 2017;16(6):566–72